International Journal of Biological Macromolecules 158 (2020) 75–84

Contents lists available at ScienceDirect

International Journal of Biological Macromolecules

journal homepage: http://www.elsevier.com/locate/ijbiomac

Cellulose nanocrystals from ultrasound process stabilizing O/W Pickering emulsion

Aureliano Agostinho Dias Meirelles [a], Ana Letícia Rodrigues Costa [b], Rosiane Lopes Cunha [a,*]

[a] Department of Food Engineering, School of Food Engineering, University of Campinas, Campinas 13083862, SP, Brazil
[b] Department of Materials and Bioprocess Engineering, School of Chemical Engineering, University of Campinas, Campinas 13083852, SP, Brazil

ARTICLE INFO

Article history:
Received 18 January 2020
Received in revised form 9 April 2020
Accepted 22 April 2020
Available online 25 April 2020

Keywords:
Cellulose
Nanocrystals
Stability of emulsions
Flaxseed oil
Ultrasound process

ABSTRACT

Cellulose nanocrystals (CNC) are bio-based solid particles arisen as promising stabilizers for Pickering emulsions in food, pharmaceutical and cosmetics industries. This study aimed to understand the stabilization mechanism of oil-in-water emulsion using CNC as stabilizing particles. CNC were obtained from cellulose microcrystalline after acid hydrolysis, dialysis, ultrasound treatment and vacuum filtration. Atomic force microscopy (AFM) showed needle-shaped CNC. The CNC presented good stability against agglomeration due to the high electrostatic repulsion between particles, making them feasible to be used in O/W emulsions. O/W emulsions were stabilized by CNC and prepared using rotor-stator and ultrasound as mechanical processes. Emulsions stabilized by CNC were opaque, homogeneous and kinetically stable during few days. Small droplets generated during the ultrasound process, could be covered by cellulose nanoparticles that acted as an effective mechanical barrier against droplets coalescence in a Pickering mechanism. The mechanism of droplets stabilization was associated with electrostatic and steric repulsion between droplets. Emulsions were evaluated varying the proportion between flaxseed oil and cellulose nanocrystals (CNC). Emulsions with a lower proportion of CNC showed better kinetic stability compared to emulsions with higher CNC proportion. After 7 days of storage, the viscosity of emulsions with a higher proportion of CNC particles decreased, which was associated to the emulsion destabilization. Our results improved the understanding of the relationship between the proportions of oil and particles for emulsion properties by evaluating the potential application of CNC as a food emulsifier.

© 2020 Elsevier B.V. All rights reserved.

1. Introduction

Consumers are increasingly aware the relationship between food consumption and a healthy lifestyle. Consumers are also concerned with environmental issues related to food processes. Therefore, the consumers appreciate products obtained from natural sources in substitution for synthetic products. Emulsions are attractive templates for new products development in order to meet this growing demand looking for new experiences of healthiness, wellness and sustainability [1].

Emulsions are present in many food products contributing to physicochemical and sensory attributes such as appearance, texture, stability, aroma, taste and mouthfeel [2]. However, emulsions are thermodynamically unstable and affected by the action of destabilizing mechanisms as aggregation, phase inversion, flocculation and coalescence [3]. Nevertheless, kinetic stability can be reached for a considerable time with the addition of emulsifiers or stabilizing particles [4].

The stability mechanism provided by solid particles is different from conventional emulsifiers. First published papers showing that particles could be used as efficient interface stabilizers were published at the beginning of the twentieth century [5,6]. Ramsden's work focused on the adsorption of organic soft solid particles called “proteids” (e.g. albumin) at air-water interfaces while Pickering showed the formation of paraffin oil-in-water (o/w) emulsions stabilized by adsorbed solid particles onto interface. Adsorption of solid particles on the oil-water interface creates a mechanical barrier protecting emulsion droplets against destabilization [7]. The strong adsorption of solid particles onto the droplet interface is caused by the partial wettability of these particles in oil and water [8].

In the last years, a growing interest in developing and applying particle-stabilized emulsions has arisen. Different inorganic particles have been studied as stabilizers for Pickering emulsions, including silica and calcium carbonate [9–11]. Bio-based solid particles have arisen as promising stabilizers for Pickering emulsions in food, pharmaceutical and cosmetics industries. The wide range and shapes of bio-based particles makes possible the preparation of Pickering emulsions with varied characteristics using fat crystals, glycerol monoleate and glyceryl stearyl citrate (diameters between 152 and 1000 nm) [12,13], polysaccharides and proteins as starch nanocrystals (diameters between 40 nm–3 μm), cellulose nanocrystals (length = 855 nm), cellulose microcrystalline (diameters between 300 nm–3 μm), chitin (240 nm × 18 nm) and chitosan (diameter between 50 and 307 nm) have been widely used as

* Corresponding author.
E-mail address: rosiane@unicamp.br (R.L. Cunha).

https://doi.org/10.1016/j.ijbiomac.2020.04.185
0141-8130/© 2020 Elsevier B.V. All rights reserved.

Pickering stabilizers [14–19]. In addition, proteins as β-lactoglobulin (diameters between 80 and 360 nm), lactoferrin (diameter between 200 and 575 nm) and soy protein isolate (diameter = 100 nm) have been also applied [20–22]. Emulsions stabilized with bio-based particles can be used to encapsulate active compounds into the internal droplet phase, control emulsion rheology by modifying particles and varying particles concentration but also to potentially replace synthetic or semi-synthetic emulsifiers avoiding some allergenic and cytotoxic effects [8,23,24].

Cellulose is the most abundant carbohydrate polymer, and materials derivate from cellulose have attracted considerable interest, especially for food-related applications [25]. Nanocelluloses are rod-like nanoparticles that can be derived from many sources such as cotton, wood, tunicate and agroindustrial-food wastes (sugarcane bagasse, mango seeds, banana peel and pineapple leaf) [26–29]. The processing conditions determine the type of nanocellulose produced: cellulose nanocrystals (CNC) are produced from chemical and enzymatic treatments, and cellulose nanofibrils (CNFs) are obtained by either mechanical or chemical treatments [30].

Cellulose nanoparticles are interesting structures for the design and development of functional nanomaterials in many applications due to several attractive features for expanding functionalization. The surface of CNCs could be modified, and used as antimicrobial agent, tissue-engineering scaffolds, biomarkers, adsorbent for water treatment and drug delivery vehicles [31–34]. Food and pharmaceutical industry could use cellulose nanoparticles as rheological and mechanical modifiers, reinforcing food-packaging films, as functional food ingredients and Pickering emulsion stabilizers [35–38].

In water-oil interfaces, cellulose nanoparticles could adsorb slower than smaller surface-active agents. However, achieved an adequate proportion of ingredients and conditions of emulsification, they may provide superior stability against aggregation and coalescence due to a strong steric repulsion [39]. Emulsions can be prepared by a number of mechanical processes, such as ultrasound treatment rotor-stator and high-pressure homogenization, to induce the mixture of oil and nanocellulose aqueous suspension promoting nanocelluloses adsorption on the oil/water interface to stabilize the emulsion [14,40–42]. In a previous work, we studied the possible mechanisms of the emulsions formation with cellulose crystals (microcrystals and nanocrystals). Cellulose crystals with different sizes contributed in different ways to the stability of the emulsions and the emulsion quality was controlled adjusting the ratio oil: particles [43]. Unlike other studies already published, in the present study the aim was to separate nanocrystals from microcrystals from the combined use of vacuum filtration and ultrasound process. To understand the mechanism of the emulsions stabilized using only cellulose nanocrystals, a study was carried out at the same time using different proportions of nanocrystals, without chemical changes in the structure of cellulose crystals, and differents proportions of flaxseed oil, a rich source of polyunsaturated fatty acids. The use of the rotor-stator and ultrasound process was used for the preparation of coarse and fine emulsions.

2. Material and methods

2.1. Material

Cellulose nanocrystals (CNC) were prepared from cellulose microcrystalline powder (20 μm) purchased from Sigma Aldrich Co. (St. Louis, EUA). Ultrapure water was obtained from a Millipore Milli-Q system (resistivity 18.2 MU/cm) and hydrochloric acid was acquired from Synth Ltda (São Paulo, Brazil). Flaxseed oil used in emulsions formulation was kindly donated by Cisbra Brasil Ltda (Rio Grande do Sul, Brazil).

2.2. Cellulose nanocrystals (CNC) preparation

CNC were obtained from cellulose microcrystalline by hydrochloric acid (HCl) hydrolysis. For this 28 g of cellulose microcrystalline was added to 1000 mL of 4 M hydrochloric acid under vigorous mechanical stirring at 80 °C during 3 h 45 min. After that, the dispersion was diluted two-fold in water and the suspension was rinsed with three repeated centrifugation cycles (15,344 g/15 min). Afterward, the bottom phase was dialyzed using dialysis tubing cellulose membrane with 12–14 kDa molecular weight cut off purchased from Sigma Aldrich Co. (St. Louis, EUA), against deionized water until dispersion reached pH 6 [44].

Cellulose crystals aqueous suspension was placed in an ultrasonic processor (QR 750 W, Ultronique, Campinas, Brazil) with a 13 mm diameter titanium probe immersed 3 mm depth. Sonication time, power and frequency were fixed at 5 min, 675 W and 20 kHz, respectively, and this process was repeated 3 times [45]. After that, aqueous suspension of cellulose crystals was subjected to vacuum filtration with filter paper showing porosity 1 μm to separate the microcrystals from the nanocrystals (CNC). Cellulose nanocrystals suspension was again subjected to ultrasound process using the same previous conditions to decrease even more the size of cellulose nanocrystals (CNC US). Particle size measurements were performed before and after this last ultrasound process.

2.3. Oil in water emulsion preparation

The oil-in-water (O/W) emulsions were prepared using different concentration of flaxseed oil (2.5%, 5% and 7.5% *w*/w) and cellulose nanocrystals (0.5% and 1.0% w/w), with a CNC concentration/oil concentration varying between 0.06 and 0.4. Coarse emulsions were prepared by homogenizing cellulose nanocrystals suspensions and flaxseed oil using a rotor-stator homogenizer Ultra Turrax model T18 (IKA, Staufen, Germany) for 3 min at 10,000 rpm (UT). The oil phase was added dropwise to the cellulose nanocrystals suspension during coarse emulsion preparation. Fine emulsions were produced from the coarse emulsion in an ultrasonic processor (QR 750 W, Ultronique, Campinas, Brazil) with a 13 mm diameter titanium probe immersed 3 mm depth. Sonication time, power and frequency were fixed at 4 min, 525 W and 20 kHz, respectively (UT + US) [46]. A cold-water bath at 10 °C was connected to the ultrasonic processor to ensure that no significant heating occurred during the homogenization process. To understand the effect of the ultrasound on the emulsification process, one condition of emulsion with flaxseed oil (2.5% *w*/w) and cellulose nanocrystals (1% w/w) was prepared using only the rotor-stator homogenizer for 3 min at 10,000 rpm and 4 min at 13,000 rpm as a control of the experiment (UT + UT).

2.4. Emulsions and particles characterization

2.4.1. Kinetic stability – laser scanning turbidimetry

Emulsion stability was measured using the optical scanning instrument Turbiscan ASG (Formulaction, Toulouse, France). The emulsions were placed in cylindrical glass tubes with screw cap (14 cm height, 1.6 cm diameter) and stored at 25 °C. The backscattered signal of the fresh emulsion (just after preparation) and stored during 15 days was scanned from the bottom to the top of the tubes with a source light at 880 nm.

2.4.2. Particles size distribution

Particles size distribution of the emulsions and CNC was determined based on the static light scattering method using a Multi-Angle Static Light-Scattering Mastersizer (Mastersizer 2000, Malvern Instruments, Worcestershire, UK). Measurements were done in triplicate, of two samples, just after emulsions preparation and 7 days after storage. The mean diameter considered as the area-surface mean diameter (D_{32}) and the polydispersity (Span) were expressed according to

Eqs. (1) and (2), respectively:

$$D_{32} = \frac{\sum nidi^3}{\sum nidi^2} \quad (1)$$

$$Span = \frac{(D_{90-}D_{10})}{D_{50}} \quad (2)$$

where n_i is the number of particles with diameter d_i, and D_{10}, D_{50} and D_{90} are diameters at 10, 50 and 90% of cumulative volume, respectively.

2.4.3. Atomic force microscopy (AFM)

The aqueous CNC suspension (1.0 μL) was placed on a grid with a mica surface and dried at room temperature to perform AFM analysis. The images were obtained with a microscope (Anasys Instruments, model nano IR2-S, Santa Barbara, United States) equipped with a camera, under controlled conditions (relative moisture = 10% and temperature = 25 °C).

2.4.4. Optical and confocal laser scanning microscopy

Optical microscopy of emulsions was performed on a Carl Zeiss Axio Scope A1 microscope (Zeiss, Oberkochen, Germany) and the images were captured with the software AxioVision Rel. 4.8 (Carl Zeiss, Germany). Confocal laser scanning microscopy was performed on a Zeiss LSM510 confocal on an Axio Observer Z.1 microscope (Carl Zeiss AG, Germany) using 40× and 100× objectives. Cellulose nanocrystals-stabilized emulsions were mixed to Congo Red and stirred for 5 min to dye the cellulose nanocrystals. Images were performed using 488 nm laser line for excitation and 605 nm emission filters for Congo Red. The confocal microscope images were analyzed with the free software ImageJ.

2.4.5. Rheological assays

Flow curves of the emulsions were obtained using a stress-controlled rheometer (AR1500ex, TA Instruments, England) using stainless steel parallel plate (diameter = 4 cm) with 1000 μm gap. Measurements were done in triplicate, of two samples, just after emulsions preparation and 7 days after storage. The analysis was done within the shear rate range between 0 and 300 s^{-1}, in three-step sequence: up-down-up. The third curve data was fitted to Newton equation (Eq. (3)).

$$\sigma = \eta\gamma \quad (3)$$

where σ is the shear stress (Pa), η is the viscosity (Pa.s) and γ is the shear rate (s^{-1}).

2.4.6. Interfacial tension

The interfacial tension between the aqueous CNC suspension and oil phase was measured before emulsion preparation by the pendant drop method using a Tracker S tensiometer (Teclis, Longessaigne, France). A syringe was used and assays were performed with the formation of a drop with 7 μL of the CNC suspension (aqueous phase) in the oil phase.

2.4.7. Zeta potential and Dynamic Light Scattering (DLS)

The zeta potential of CNC suspended in Milli-Q water (0.01% *w*/w) was determined in triplicate, of two samples, in a Nano-ZS Zetasizer equipment (Malvern Instruments, Worcestershire, UK). DLS measurements were carried out at 173° scattering angle after equilibrating CNC aqueous suspensions (0.1% w/w) at 25 °C for 10 min. Mean particle size was reported as the average hydrodynamic diameter (D), which was calculated according to the Stokes-Einstein relation (Eq. (4)) for rod-shaped particles [47].

$$D = \frac{KT}{3\pi\eta D_t} \quad (4)$$

where K is Boltzmann's constant ($J.K^{-1}$), T is the absolute temperature (K), η is the viscosity (Pa.s) and D_t is the translational diffusion coefficient (m^2/s). The polydispersity index (PDI) was calculated from cumulant analysis of the intensity autocorrelation function of measured dynamic light scattering.

2.4.8. Statistical analysis

Analysis of variance (ANOVA) was performed using the software STATISTICA 7.0 (Statsoft Inc., Tulsa, USA) and significant differences ($p < 0.05$) between the treatments were evaluated using Tukey test.

3. Results and discussion

3.1. Effect of the ultrasound process on the preparation of cellulose nanocrystals

Fig. 1 shows the visual appearance of cellulose nanoparticles and distilled water for comparative effect. Flasks 2 and 3 are suspensions containing 0.5% *w*/w cellulose nanocrystals, while flasks 4 and 5 contained 1% w/w cellulose nanocrystals. Flasks 3 and 5 contained cellulose nanocrystals after additional ultrasound treatment. In general, more concentrated dispersions (1% *w*/w) presented higher turbidity when compared with the less concentrated samples (0.5% w/w). Ultrasound-treated samples also showed slightly higher turbidity when compared to the untreated samples. Turbid dispersions were not expected considering that cellulose particles are nanometric and

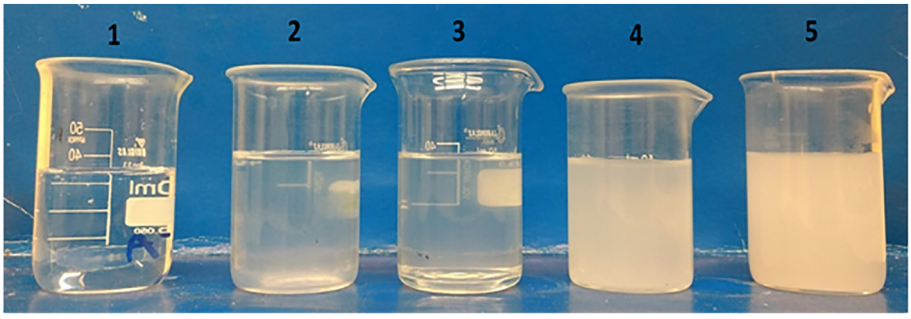

Fig. 1. Visual appearance of suspensions of cellulose nanocrystals prepared in different conditions and compared with distilled water.

thus additional measurements were performed to understand this behavior.

Atomic force microscopy (AFM) obtained for untreated cellulose microcrystalline (from Sigma-Aldrich) and cellulose nanocrystals (CNC) are presented in Fig. 2. Our results show that microcrystalline cellulose, before all treatments, shows an agglomerate with large size (higher than 10 μm). However, CNC dispersed in more separate networks were observed after the acid treatment, centrifugation, dialysis, vacuum filtration and an additional step of ultrasound process, characteristic of cellulose nanocrystals. The morphology obtained was needle-like showing that the isolation of cellulose microcrystalline to CNC was successfully done [48,49]. Although the lower dimension of CNC was nanometric, the length of the nanocrystals was higher than 1 μm explaining at least partly the turbidity of the suspensions.

Table 1 shows the properties of cellulose crystals dispersed in water after vacuum filtration, before and after to be subjected to the ultrasound process. In a previous paper, we observed that the hydrolysis process reduced the microcrystalline cellulose size approximately four times, up to 5 μm, with initial cellulose crystals presenting a mean diameter around 20 μm. In addition, a bimodal particle size distribution was identified, which indicated that the process was not efficient enough to produce only nanoparticles [43]. To prepare cellulose nanocrystals from the mixture of cellulose micro/nanocrystals, cellulose crystals were subjected to ultrasound process (675 W/5 min/3×), vacuum filtration and an additional step of ultrasound process (675 W/5 min). In the first and third line of Table 1, it is possible to observe that the application of the ultrasound process and the vacuum filtration was not sufficient to produce only nanoparticles (CNC), since some cellulose microcrystals were even observed after vacuum filtration. The application of one more step of the ultrasound process was useful to produce cellulose nanocrystals (CNC US), as can be observed in the second and fourth line of Table 1 (microparticles were not identified). After the ultrasound treatment, no significant difference was observed in mean particle size of the cellulose nanocrystals. In addition, the polydispersity (PDI) of the cellulose crystals decreased after the ultrasound treatment, indicating greater uniformity of cellulose crystals size as the medium to high-intensity ultrasound power applied in short periods helps to break down cellulosic structures [16].

Electrostatic stability of cellulose crystals was determined by the zeta potential values (Table 1). Cellulose crystals after the ultrasound process and vacuum filtration showed good stability against agglomeration with values between −24 and −27 mV. The use of an additional ultrasound process step induced an increase in the zeta potential of cellulose nanocrystals with values between −31 and −33 mV. In this later condition, the suspensions presented great stability since a stable suspension of cellulose crystals should have a zeta potential value lesser than −30 mV or >25–30 mV [50–52]. One more step of ultrasound process promoted regions of hydrodynamic shear close to the tip of the probe and greater chaotic contact between cellulose particles and oxygen, favoring the generation of more negative charge on cellulose crystals surface due to the partial break of the particles [24,26].

Interfacial tension measurements were performed to understand the role of CNC particles on the stabilization mechanism of oil-in-water emulsions (Fig. 3). The interfacial tension between the flaxseed oil droplet and distilled water was measured as a control experiment (*blank*). Values of the initial interfacial tension of the three systems (water, CNC and CNC US) were similar, close to 20mN/m, but interfacial tension showed a progressive decrease over time. After 2000 s, the equilibrium was reached for all systems and equilibrium tension between water and flaxseed oil was low, <10 mN/m, which was also observed by other authors [53,54]. In addition, CNC did not contribute to the reduction of interfacial tension between water and flaxseed oil, since results of all systems were similar and equilibrium interfacial tension was around 8 mN/m, including with water as aqueous phase, indicating that the mechanism for emulsion stabilization produced with these particles differs from the conventional emulsifiers [3,55]. In Pickering emulsion stabilization, the interfacial tension is not expected to be widely influenced by the presence of particles [39]. In addition, the rod-shaped cellulose nanocrystals used to stabilize emulsions were flexible enough to surround at the droplet surface, resulting in an efficient interfacial coating [56]. Considering these aspects, we could infer that cellulose nanocrystals stabilized emulsions by Pickering and electrostatic mechanism.

3.2. Different proportions of cellulose nanocrystals and flaxseed oil change the properties of the Pickering emulsions

The visual appearance of CNC-stabilized emulsions is presented in Fig. 4, immediately after preparation, after one day of storage and after 7 days of storage at room temperature. All the fresh emulsions were opaque, homogeneous and showed only one phase. After one day of storage, emulsions also showed one continuous homogeneous phase. However, after 7 days of storage, emulsions were not homogeneous, showing a clarified layer with a small amount of sedimented CNC particles in the bottom of the measuring cell of the emulsion with 2.5% (*w*/w) of flaxseed oil. In addition, after 7 days of storage, a formation of a slight interface could be observed at the top of the measuring cell with 7.5% (w/w) of flaxseed oil.

Kinetic stability of the emulsions was determined after 0 (fresh emulsion), 1, 3, 7 and 15 days of storage at 25 °C. Emulsion stability

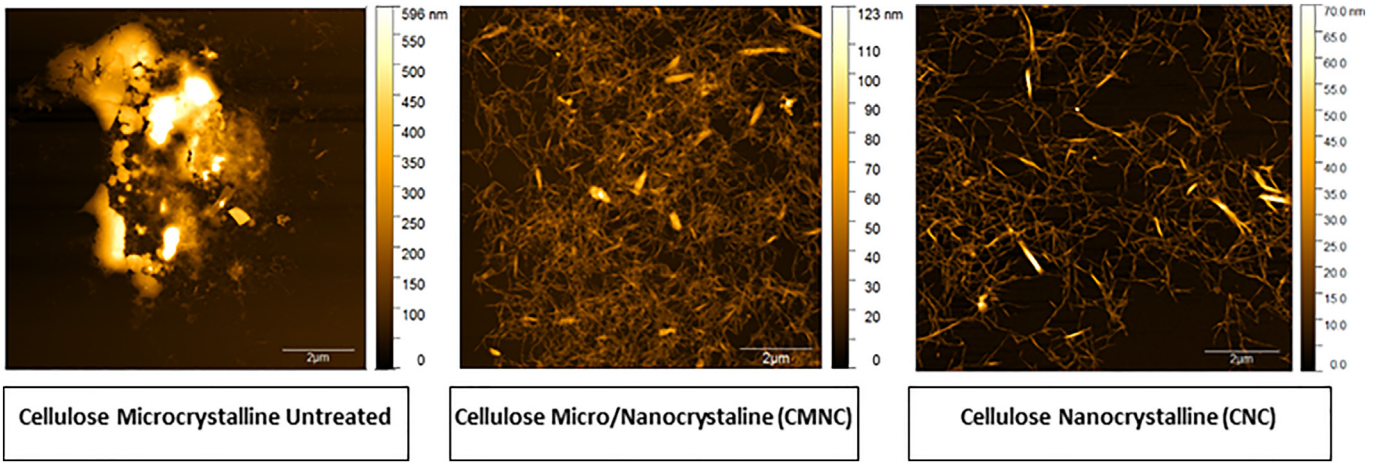

Fig. 2. AFM images of the untreated cellulose microcrystalline (left), cellulose micro/nanocrystalline (CMNC) after the acid treatment, centrifugation and dialysis (middle) and cellulose nanocrystalline (CNC) after the acid treatment, centrifugation, dialysis vacuum filtration and an additional step of ultrasound process (right) (scanning area 10.0 μm × 10.0 μm, scale bar = 2 μm).

Table 1
Properties of cellulose crystals dispersed in water after vacuum filtration before and after to be subjected to ultrasound process.

CNC (%/w/w)	Ultrasound condition	Particle size distribution				Zeta potential (mV)	pH
		Mastersizer - Static light scattering measurement		Zetasizer - Dynamic Light Scattering measurement			
		D_{32}/μm (Volume Distribution)	Span	D/nm (Intensity Distribution)	PDI		
0.5	–	4.89 ± 0.05[a]	2.64 ± 0.15[a]	400.13 ± 17.38[b]	0.73 ± 0.02[d]	−24.61 ± 0.65[a]	6.52 ± 0.02[b]
0.5	675 W/5 min	n.i	n.i	326.88 ± 26.26[a]	0.29 ± 0.05[a]	−31.54 ± 1.08[c]	6.39 ± 0.04[a]
1	–	5.57 ± 0.02[b]	4.95 ± 0.66[b]	527.41 ± 56.83[c]	0.52 ± 0.02[c]	−27.72 ± 0.86[b]	6.77 ± 0.06[c]
1	675 W/5 min	n.i	n.i	315.46 ± 65.01[a]	0.37 ± 0.02[b]	−33.41 ± 1.22[c]	6.63 ± 0.03[c]

Different letters in the same column indicate significant difference at $p < 0.05$. n.i = not identified.

can be referred as the resistance of an emulsion to the properties changes over time. The multiple light scattering technique provides information about the changes associated with destabilization phenomenon even before the visual phase separation. The backscattering (BS) profiles versus the height of the measuring cell are shown in Fig. 5. Immediately after the homogenization process (Day 0, black lines), BS values increased rapidly, between 0 and 5 mm, due to the edge effect of the measuring cell. After 5 mm of height, BS values only varied slightly as a function of the height of the measuring cell since droplets were uniformly dispersed throughout the system. BS values were inversely proportional to the droplet size as the fresh emulsions produced using only rotor-stator presented BS values around 30% and bigger droplets mean size (~3 μm), while the fresh emulsions produced from ultrasound process showed BS values around 45–70%, and smaller droplets mean size (1.36–1.69 μm) (Table 2). On the other hand, fresh emulsions prepared with flaxseed oil and a mixture of cellulose micro and nanocrystals, using only rotor-stator were more stable presenting BS values around 60% with larger droplets mean size (5.41 μm), while the fresh emulsions produced from ultrasound process showed BS values around 70–80%, with smaller droplets mean size (1.96–2.59 μm) [43].

During storage, BS values (orange, gray, yellow and red lines) changed and BS values increased more slowly to the top of the measuring cell. For a same cell height, the BS decreased over the days. For example, evaluating the same height of 20 mm of emulsion with 0.5% CNC and 5% oil, the fresh emulsion showed BS value around 66%, after 7 days of storage the BS value was 50% and after 15 days of storage BS value was 42%. This backscattering data profile indicates that the emulsion clarified, according to the signal decrease on the bottom of the cell measurement [57]. The droplets, which were initially dispersed uniformly in the emulsified systems, migrated and became more concentrated at the top-measuring cell promoting the increase of BS values. A pronounced increase (steep-slope) of the BS values, indicates the presence of a defined interface (clarified serum and/or cream layer) which was observed for most of the emulsions. The amount of CNC exerted influence on the emulsion behavior, since densely covered emulsion surfaces are formed by short nanocrystals, whereas long CNC rod shape form less covered surfaces [40]. However, emulsions containing 1% (w/w) CNC and 2.5% (w/w) oil showed that the amount of cellulose crystals was in excess to prevent the system destabilization ($r = 0.4$). Some works associated creaming phenomenon with the bridging

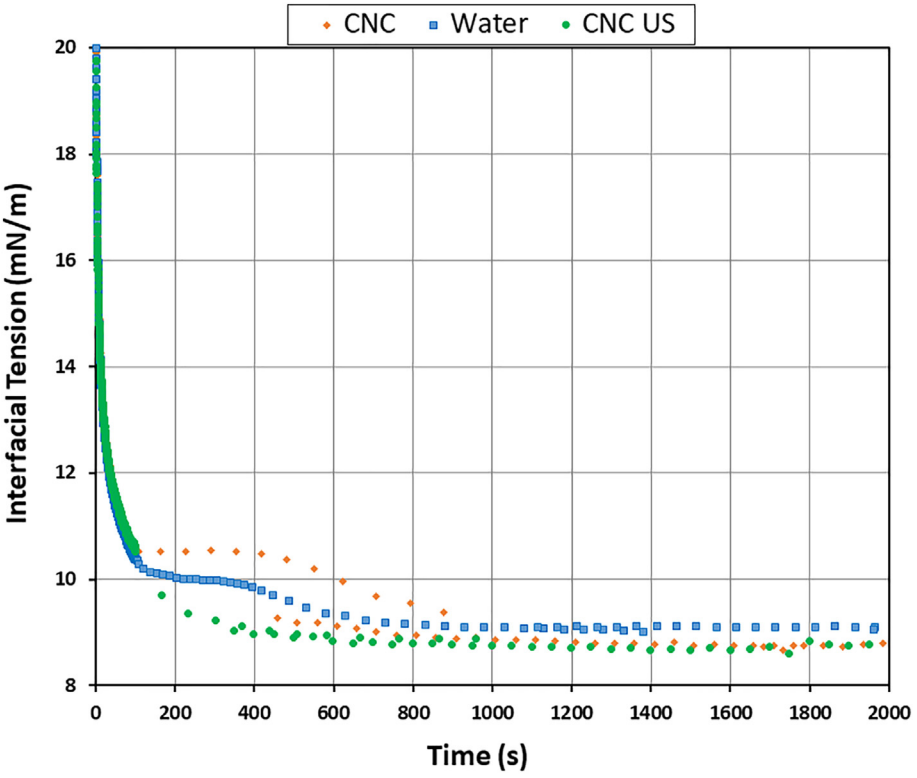

Fig. 3. Dynamic interfacial tension between flaxseed oil and water or cellulose nanocrystals (CNC) aqueous suspensions. CNC were obtained after different process conditions using vacuum filtration (1 μm) to separate the microcrystals from the nanocrystals (CNC) or after vacuum filtration and ultrasonic treatment (CNC US).

Fig. 4. Visual appearance of fresh emulsions, after one day and 7 days of storage, stabilized with different proportions of cellulose nanocrystals (CNC) homogenized by rotor-stator and ultrasound process (UT + US). Condition with * is an emulsion produced only with rotor stator process (UT + UT). Red arrows indicate the point of interface formation or phase separation.

flocculation of cellulosic particles in emulsified systems due to interparticles hydrophobic interactions, electrostatic repulsion and van der Waals forces [58,59]. Moreover, our results suggest a slow creaming rate during the days of storage due to the small droplets formed, which could be associated with the fast deposition of CNC onto the droplets interface during emulsification using rotor-stator and ultrasound process.

The oil concentration is an important factor for the stability of the emulsions, since for the same concentration of CNC particles, the increase of the oil content increased the BS values for fresh emulsions (Day 0, black lines), which means that a better proportion between CNC and oil could be achieved. As aforementioned even 1.0% (*w*/w) of CNC may be used in excess (with 2.5% oil), i.e., the CNC covered the oil droplets and the excess was dispersed into the aqueous phase of the system. Part of CNC sedimented and a clarified layer was produced at the bottom of the sample (Fig. 4). At the same time, other phenomena were observed in emulsions with 1% CNC, sedimentation (5% w/w oil) and creaming (7.5% w/w oil) (Fig. 4/ Fig. 5). From another point of view, emulsions with the same ratio (CNC concentration/oil concentration) $r = 0.2$, with 5% w/w oil were more stable during storage time, with higher BS values and smaller clarified region in the measuring cell (Figs. 4 and 5). Emulsions with ratios of 0.06, 0.1 and 0.2 with 0.5% (*w*/w) of CNC showed better kinetic stability compared to emulsions with 1% (w/w) of CNC. The ratio (CMNC concentration/oil concentration) was an import parameter to understand the stability of emulsions prepared with flaxseed oil and cellulose micro and nanocrystals (CMNC). Emulsions with the lowest ratios (0.13–0.25) were more stable over time [43], as observed in the present work showing the relevance of the ratio CNC/oil.

Microscopic pictures (fresh emulsion) and corresponding particle size distribution (D_{32}) was determined for fresh emulsion and on the 7th day of storage (Fig. 6). Fresh emulsion produced using only rotor-stator presented a bimodal particle size distribution, with the highest mean values of droplet size (around 3 μm) and polydispersity. Fresh emulsion produced using the rotor-stator followed by the ultrasound process showed monomodal size distribution, with smaller mean droplet size values. A monodisperse droplet size distribution associated with smaller droplet mean diameter reduces (or delays) the occurrence of destabilization mechanisms and indicates enhanced stability of the emulsion [57]. Comparing both processes rotor-stator (UT + UT) and ultrasound (UT + US), the later reduced the droplet size in 50% using the same emulsion condition (1% *w*/w CNC and 2.5% w/w flaxseed oil). The microscopies of the fresh emulsions confirm that there is no presence of large cellulose crystals contributing to the emulsions stability.

In a previous paper, flaxseed oil emulsions stabilized with cellulose crystals prepared with ultrasound process presented a bimodal particle size distribution with bigger droplet size values (around 1.96–2.59 μm) and higher polydispersity. Micro and nanoparticles of cellulose formed a network in the continuous phase, immobilizing the oil droplets and enhancing physical stability [43] in comparison to results of the present work that only nanoparticles stabilized emulsions. In addition, emulsions with CNC particles (0.75% *w*/w) and (10% w/w) flaxseed oil produced with high energy microfluidizer showed monomodal

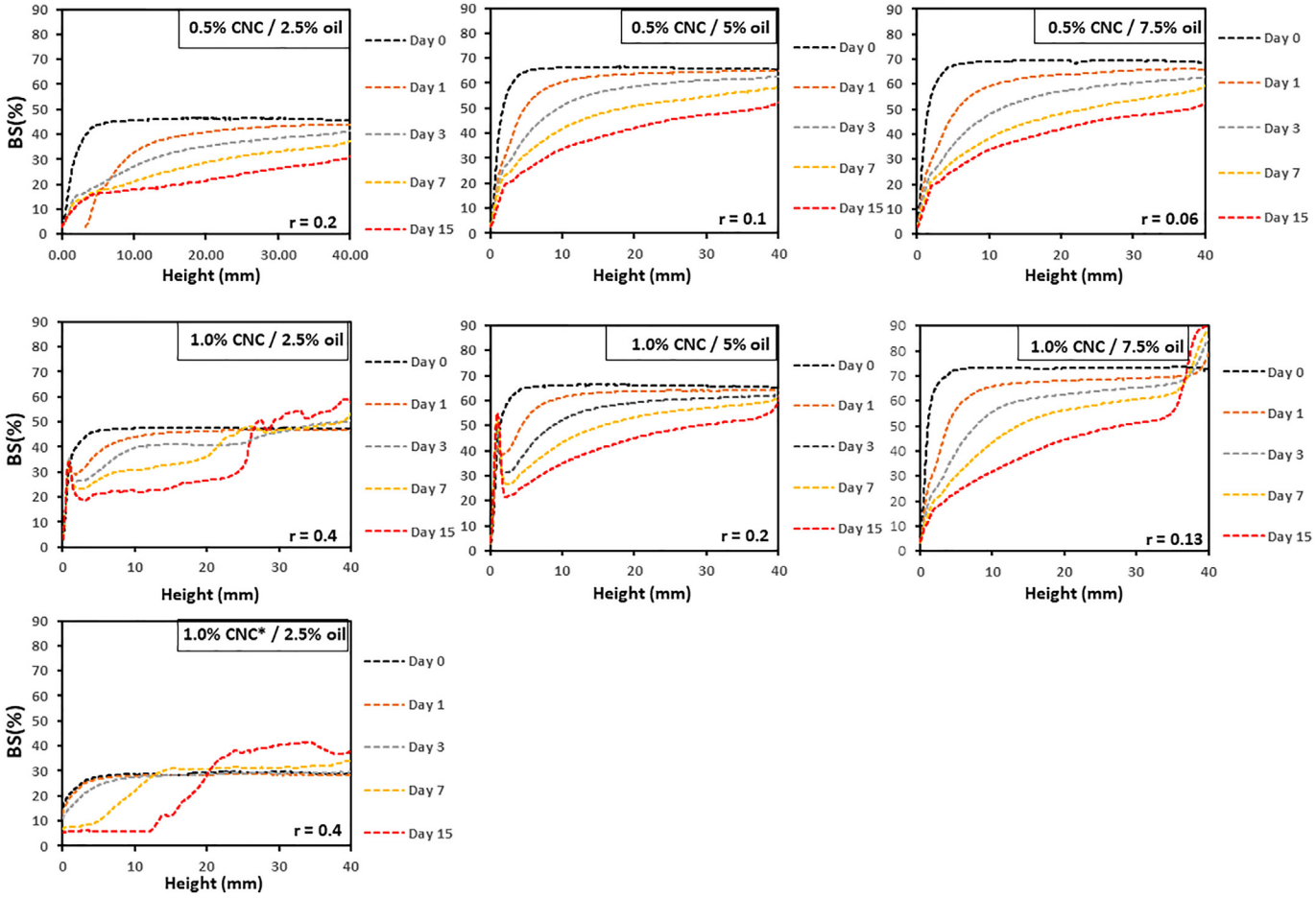

Fig. 5. Backscattering profiles (0, 1, 3, 7, and 15 days of storage) of emulsions stabilized with different proportions of cellulose nanocrystals (CNC) homogenized by ultrasound process (UT + US). r = ratio between CNC and oil concentration. Condition with * is an emulsion produced only with rotor stator process (UT + UT).

distribution and smaller droplet sizes (0.5–0.7 μm) [60] compared to our results, which could be attributed to the higher oil content of the former.

Table 2 shows the mean droplet size (D_{32}) and polydispersity index (Span) of the emulsions. The values of droplets size (D_{32}) ranged from 1.21–3.42 μm and Span ranged from 1.25–4.09. Fresh emulsions showed a tendency to increase droplet size as the CNC concentration increased, keeping fixed the oil concentration (Table 2). On the other hand, droplet size remained constant when the oil concentration was increased, for 2.5% to 5% (*w*/w) of oil, keeping fixed the CNC concentration. However, there was a small significant increase in droplet size in emulsions with 7.5% (w / w) of flaxseed oil, keeping fixed the CNC concentration (Table 2). Higher oil content makes difficult small droplets formation and promotes greater proximity between them, favoring the coalescence, flocculation or agglomeration of droplets [3], which was confirmed by microscopy (Fig. 6).

Rheological properties of emulsions with different concentrations of cellulose particles and oil were well-fitted to Newton equation. All emulsions showed liquid-fluid appearance during the days of storage. A slightly higher viscosity was observed for the emulsions produced using the ultrasound process, compared to the rotor-stator process (Table 3). The viscosity of the fresh emulsions increased as the oil content increased, keeping fixed the CNC concentration, because a higher number of droplets increases the energy dissipation associated with fluid flow. At the same time, the viscosity increased when the CNC concentration was increased, keeping fixed the oil concentration, except for the emulsion produced only with rotor-stator process, due to the emulsion instability. After 7 days of storage, the viscosity did not show

Table 2
Droplets size of emulsions produced from different mechanical processes and ratio between CNC and oil concentration.

Process	CNC (% w/w)	2.5% oil (*w*/w)				5% oil (w/w)				7.5% oil (*w*/w)			
		0 day		7th day (cream phase)		0 day		7th day (cream phase)		0 day		7th day (cream phase)	
		D_{32} (μm)	Span	D_{32} (μm)	Span	D_{32} (μm)	Span	D_{32} (μm)	Span	D_{32} (μm)	Span	D_{32} (μm)	Span
UT + US	0.5	1.36 ± 0.11^{Aab}	1.41 ± 0.16^{Ae}	1.21 ± 0.07^{Aa}	1.51 ± 0.23^{Ae}	1.36 ± 0.05^{Aab}	1.42 ± 0.06^{Ae}	1.59 ± 0.12^{Acd}	1.79 ± 0.12^{Af}	1.62 ± 0.03^{Ad}	1.53 ± 0.17^{Ae}	1.43 ± 0.03^{Abc}	1.47 ± 0.19^{Ae}
	1.0	1.50 ± 0.02^{Ba}	1.42 ± 0.20^{Acd}	1.47 ± 0.02^{Ba}	1.69 ± 0.18^{Ad}	1.55 ± 0.04^{Ba}	1.25 ± 0.03^{Bc}	1.45 ± 0.14^{Aa}	2.13 ± 0.06^{Be}	1.69 ± 0.18^{Ab}	1.31 ± 0.07^{Bc}	1.66 ± 0.08^{Bb}	3.01 ± 0.56^{Bf}
UT + UT	1	2.97 ± 0.04^{Ca}	3.25 ± 0.05^{Bc}	3.42 ± 0.05^{Cb}	4.09 ± 0.21^{Bd}	–	–	–	–	–	–	–	–

Different letters indicate significant difference at $p < 0.05$ for the same property. Small letters: differences in the same line between the storage time. Capital letters: differences in the same column between CNC concentration.

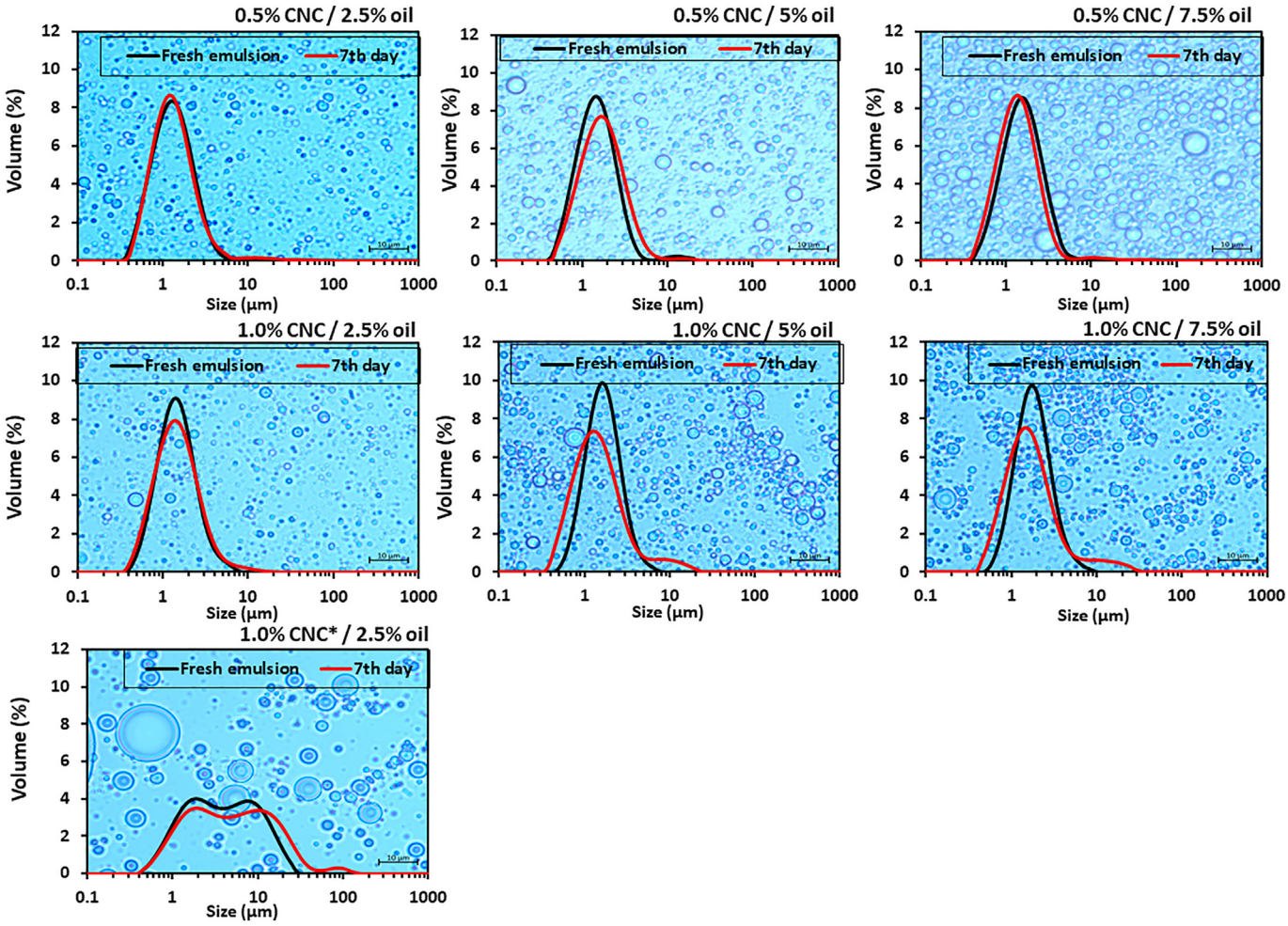

Fig. 6. Particle size distribution of fresh emulsions and after 7 days of storage. Background: micrographs of fresh emulsions stabilized with different proportions of cellulose nanocrystals (CNC) homogenized by rotor-stator and ultrasound process (UT + US). Condition with * is an emulsion produced only with rotor stator process (UT + UT).

significant difference with emulsions 0.5% (*w*/w) of CNC particles, regardless of the proportion of oil used. However, the viscosity decreased for emulsions with 1% (w/w) of CNC, which could be associated to the emulsion destabilization. Emulsion prepared with corn oil (10% w/w) and different CNC concentrations, between 0.2 and 2% (w/w) were also well-fitted to Newton equation and showed the same behavior with the increase of CNC concentration. In addition, emulsions with >1% (w/w) CNC showed less liquid appearance [60].

Confocal micrographs showed the cellulose nanocrystals (red/green color) distribution onto the emulsion droplets (Fig. S1, supplementary materials). We had a limitation of the visualization due to the characteristics of the emulsions and equipment capacity associated to the small droplets generated during the ultrasound process with cellulose nanoparticles (Fig. 6). The confocal images showed that the oil droplets remained as individual entities and were evenly spread while the visualization of a large number of nanocrystals dispersed was possible (small green and red points dispersed throughout the image). Immediately after emulsion preparation, we believe that occurred the formation of a thick CNC assembly around the droplet surfaces, inducing steric hindrance (Pickering mechanism), but also a contribution of electrostatic repulsion due to the negative charge of the CNC-coated oil droplets [61–63].

4. Conclusions

The effect of the ultrasound process and proportion of oil:cellulose nanocrystals particles (CNC) on the emulsion properties were studied. Ultrasound associated with vacuum filtration allowed the production of cellulose particles with monomodal distribution in nanometric scale that were used to emulsion stabilization. CNC did not contribute to the reduction of interfacial tension between water and flaxseed oil, which was expected in Pickering emulsions. After emulsion preparation,

Table 3
Viscosity of emulsions, produced by different processes and ratio between CNC and oil concentration.

Process	CNC (%, w/w)	2.5% oil (w/w)		5% oil (w/w)		7.5% oil (w/w)	
		η (mPa.s)		η (mPa.s)		η (mPa.s)	
		0 day	7th day	0 day	7th day	0 day	7th day
UT + US	0.5	1.45 ± ˙0.01^{aA}	1.42 ± 0.02^{aA}	1.52 ± 0.02^{bA}	1.49 ± ˙0.01^{abB}	1.72 ± ˙0.01^{cA}	1.68 ± 0.03^{cA}
	1	1.57 ± 0.02^{bB}	1.49 ± ˙0.01^{aA}	1.68 ± 0.05^{cB}	1.52 ± ˙0.01^{aB}	1.88 ± 0.03^{dB}	1.71 ± ˙0.01^{cB}
UT + UT	1	1.32 ± ˙0.01^{aC}	1.25 ± ˙0.01^{bB}	–	–	–	–

Different letters indicate significant difference at $p < 0.05$. Small letters: differences in the same line. Capital letters: differences in the same column.

smaller crystals covered flaxseed oil droplets but the effect of the proportion between the concentration of cellulose particles and flaxseed oil was relevant for stabilizing properties. Emulsions with 0.5% (w/w) of CNC showed better kinetic stability compared to emulsions with CNC 1% (w/w). Emulsions showed Newtonian behavior with low viscosity. After 7 days of storage, the viscosity did not show significant difference in emulsions with 0.5% (w/w) of CNC particles but viscosity decreased for emulsions with 1% (w/w) of CNC that could be associated to the emulsion destabilization. It was clear that the ultrasound process improved emulsions stability, which showed higher kinetic stability, with monomodal droplet size distribution and slight higher emulsion viscosity. We expect that the results could provide relevant findings about how different proportions of CNC nanoparticles and flaxseed oil could produce emulsion with varied characteristics.

Supplementary data to this article can be found online at https://doi.org/10.1016/j.ijbiomac.2020.04.185.

Author contributions

Aureliano Agostinho Dias Meirelles: conceptualization, methodology, investigation, writing (original draft) and formal analysis; Ana Letícia Rodrigues Costa: conceptualization, methodology, investigation, writing (original draft) and formal analysis; Rosiane Lopes Cunha: conceptualization, writing (review and editing), supervision, funding acquisition.

Acknowledgments

The authors acknowledge the financial support received from FAPESP – São Paulo - Brazil for the financial support (Process numbers 2007/58017-5 and 2011/06083-0). This study was financed in part by the Coordenação de Aperfeiçoamento de Pessoal de Nível Superior – Brasil (CAPES) – Financial code 001. Aureliano Agostinho Dias Meirelles thanks CAPES – Brazil for the PhD fellowship. Ana Letícia Rodrigues Costa Lelis thanks CNPq – Brazil (CNPq 154160/2018-0). Rosiane Lopes Cunha thanks CNPq – Brazil (CNPq 307168/2016-6) for the productivity grant. The authors thank the Laboratory for Surface Science (LCS) of the National Nanotechnology Laboratory (LNNano) (Campinas, Brazil) for AFM analyses.

References

[1] J. Toledo Guimarães, E.K. Silva, M.Q. Freitas, M.A.A. Meireles, A.G. Cruz, Non-thermal emerging technologies and their effects on the functional properties of dairy products, Curr. Opin. Food Sci. 22 (2018) 62–66.
[2] D.J. McClements, C.E. Gumus, Natural emulsifiers — biosurfactants, phospholipids, biopolymers, and colloidal particles: molecular and physicochemical basis of functional performance, Adv. Colloid Interf. Sci. 234 (2016) 3–26.
[3] D.J. McClements, Food Emulsions: Principles, Practices, and Techniques, 2° ed. CRC Press, Washington, D.C, 2005.
[4] D.J. McClements, Critical review of techniques and methodologies for characterization of emulsion stability, Crit. Rev. Food Sci. Nutr. 47 (7) (2007) 611–649.
[5] W. Ramsden, F. Gotch, Separation of solids in the surface-layers of solutions and suspensions (observations on surface-membranes, bubbles, emulsions, and mechanical coagulation) - preliminary account, Royal Society 72 (477–486) (1904) 156–164.
[6] S.U. Pickering, CXCVI.-emulsions, J. Chem. Soc. 91 (1907) 2001–2021.
[7] E. Dickinson, Food emulsions and foams: stabilization by particles, Curr. Opin. Colloid Interface Sci. 15 (1–2) (2010) 40–49.
[8] Y. Chevalier, M.-A. Bolzinger, Emulsions stabilized with solid nanoparticles: Pickering emulsions, Colloids Surf. A Physicochem. Eng. Asp. 439(0) (2013) 23–34.
[9] B.P. Binks, S.O. Lumsdon, Pickering emulsions stabilized by monodisperse latex particles: effects of particle size, Langmuir 17 (15) (2001) 4540–4547.
[10] B.P. Binks, J. Philip, J.A. Rodrigues, Inversion of silica-stabilized emulsions induced by particle concentration, Langmuir 21 (8) (2005) 3296–3302.
[11] Z.G. Cui, K.Z. Shi, Y.Z. Cui, B.P. Binks, Double phase inversion of emulsions stabilized by a mixture of CaCO3 nanoparticles and sodium dodecyl sulphate, Colloids Surf. A Physicochem. Eng. Asp. 329 (1) (2008) 67–74.
[12] S. Ghosh, T. Tran, D. Rousseau, Comparison of Pickering and network stabilization in water-in-oil emulsions, Langmuir 27 (11) (2011) 6589–6597.
[13] R. Gupta, D. Rousseau, Surface-active solid lipid nanoparticles as Pickering stabilizers for oil-in-water emulsions, Food Funct. 3 (3) (2012) 302–311.
[14] I. Kalashnikova, H. Bizot, B. Cathala, I. Capron, New Pickering emulsions stabilized by bacterial cellulose nanocrystals, Langmuir 27 (12) (2011) 7471–7479.
[15] M. Kargar, K. Fayazmanesh, M. Alavi, F. Spyropoulos, I.T. Norton, Investigation into the potential ability of Pickering emulsions (food-grade particles) to enhance the oxidative stability of oil-in-water emulsions, J. Colloid Interface Sci. 366 (1) (2012) 209–215.
[16] C. Li, P. Sun, C. Yang, Emulsion Stabilized by Starch Nanocrystals, 64(6), 2012 497–502.
[17] H. Liu, C. Wang, S. Zou, Z. Wei, Z. Tong, Simple, reversible emulsion system switched by pH on the basis of chitosan without any hydrophobic modification, Langmuir 28 (30) (2012) 11017–11024.
[18] M.V. Tzoumaki, T. Moschakis, V. Kiosseoglou, C.G. Biliaderis, Oil-in-water emulsions stabilized by chitin nanocrystal particles, Food Hydrocoll. 25 (6) (2011) 1521–1529.
[19] I. Tavernier, W. Wijaya, P. Van der Meeren, K. Dewettinck, A.R. Patel, Food-grade particles for emulsion stabilization, Trends Food Sci. Technol. 50 (2016) 159–174.
[20] M. Destribats, M. Rouvet, C. Gehin-Delval, C. Schmitt, B.P. Binks, Emulsions stabilised by whey protein microgel particles: towards food-grade Pickering emulsions, Soft Matter 10 (36) (2014) 6941–6954.
[21] G. Shimoni, C. Shani Levi, S. Levi Tal, U. Lesmes, Emulsions stabilization by lactoferrin nano-particles under in vitro digestion conditions, Food Hydrocoll. 33 (2) (2013) 264–272.
[22] F. Liu, C.-H. Tang, Soy protein nanoparticle aggregates as Pickering stabilizers for oil-in-water emulsions, J. Agric. Food Chem. 61 (37) (2013) 8888–8898.
[23] J. Wu, G.H. Ma, Recent studies of Pickering emulsions: particles make the difference, Small (Weinheim an Der Bergstrasse, Germany) 12 (34) (2016) 4633–4648.
[24] A.L.R. Costa, A. Gomes, G.d.F. Furtado, H. Tibolla, F.C. Menegalli, R.L. Cunha, Modulating in vitro digestibility of Pickering emulsions stabilized by food-grade polysaccharides particles, Carbohydr. Polym. 227 (2020), 115344.
[25] D. Klemm, B. Heublein, H.P. Fink, A. Bohn, Cellulose: fascinating biopolymer and sustainable raw material, Angewandte Chemie (International Ed. in English) 44 (22) (2005) 3358–3393.
[26] A.L.R. Costa, A. Gomes, H. Tibolla, F.C. Menegalli, R.L. Cunha, Cellulose nanofibers from banana peels as a Pickering emulsifier: high-energy emulsification processes, Carbohydr. Polym. 194 (2018) 122–131.
[27] M.A. Henrique, H.A. Silvério, W.P. Flauzino Neto, D. Pasquini, Valorization of an agro-industrial waste, mango seed, by the extraction and characterization of its cellulose nanocrystals, J. Environ. Manag. 121 (2013) 202–209.
[28] S. Saha, R. Ghosh, Cellulose nanocrystals from lignocellulosic agro-waste: a comparative study on conventional and ultrasonic assisted preparation methods, Materials Today: Proceedings 11 (2019) 628–636.
[29] R.M.d. Santos, W.P. Flauzino Neto, H.A. Silvério, D.F. Martins, N.O. Dantas, D. Pasquini, Cellulose nanocrystals from pineapple leaf, a new approach for the reuse of this agro-waste, Ind. Crop. Prod. 50 (2013) 707–714.
[30] N. Grishkewich, N. Mohammed, J. Tang, K.C. Tam, Recent advances in the application of cellulose nanocrystals, Curr. Opin. Colloid Interface Sci. 29 (Supplement C) (2017) 32–45.
[31] Y. Zhou, S. Sun, W. Bei, M.R. Zahi, Q. Yuan, H. Liang, Preparation and antimicrobial activity of oregano essential oil Pickering emulsion stabilized by cellulose nanocrystals, Int. J. Biol. Macromol. 112 (2018) 7–13.
[32] W. Luo, L. Cheng, C. Yuan, Z. Wu, G. Yuan, M. Hou, J.Y. Chen, C. Luo, W. Li, Preparation, characterization and evaluation of cellulose nanocrystal/poly(lactic acid) in situ nanocomposite scaffolds for tissue engineering, Int. J. Biol. Macromol. 134 (2019) 469–479.
[33] M. Ma, Z. Liu, L. Hui, Z. Shang, S. Yuan, L. Dai, P. Liu, X. Liu, Y. Ni, Lignin-containing cellulose nanocrystals/sodium alginate beads as highly effective adsorbents for cationic organic dyes, Int. J. Biol. Macromol. 139 (2019) 640–646.
[34] J.T. Orasugh, G. Sarkar, N.R. Saha, B. Das, A. Bhattacharyya, S. Das, R. Mishra, I. Roy, A. Chattoapadhyay, S.K. Ghosh, D. Chattopadhyay, Effect of cellulose nanocrystals on the performance of drug loaded in situ gelling thermo-responsive ophthalmic formulations, Int. J. Biol. Macromol. 124 (2019) 235–245.
[35] H. Yan, X. Chen, M. Feng, Z. Shi, W. Zhang, Y. Wang, C. Ke, Q. Lin, Entrapment of bacterial cellulose nanocrystals stabilized Pickering emulsions droplets in alginate beads for hydrophobic drug delivery, Colloids Surf. B: Biointerfaces 177 (2019) 112–120.
[36] L. Wang, C. Chen, J. Wang, D.J. Gardner, M. Tajvidi, Cellulose nanofibrils versus cellulose nanocrystals: comparison of performance in flexible multilayer films for packaging applications, Food Packag. Shelf Life 23 (2020), 100464.
[37] Y. Wang, R. Xie, D. Li, Y. Shen, W. Xie, H. Wang, L. Gan, J. Huang, A cross-linking/percolating-integrated strategy to enhance crystallizable rubber using rod-like reactive biobased nanocrystals, ACS Applied Bio Materials 3 (1) (2020) 441–449.
[38] R. Mu, X. Hong, Y. Ni, Y. Li, J. Pang, Q. Wang, J. Xiao, Y. Zheng, Recent trends and applications of cellulose nanocrystals in food industry, Trends Food Sci. Technol. 93 (2019) 136–144.
[39] C.C. Berton-Carabin, K. Schroën, Pickering emulsions for food applications: background, trends, and challenges, Annu. Rev. Food Sci. Technol. 6 (1) (2015) 263–297.
[40] I. Kalashnikova, H. Bizot, P. Bertoncini, B. Cathala, I. Capron, Cellulosic nanorods of various aspect ratios for oil in water Pickering emulsions, Soft Matter 9 (3) (2013) 952–959.
[41] I. Kalashnikova, H. Bizot, B. Cathala, I. Capron, Modulation of cellulose nanocrystals amphiphilic properties to stabilize oil/water Interface, Biomacromolecules 13 (1) (2012) 267–275.
[42] K.P. Oza, S.G. Frank, Microcrystalline cellulose stabilized emulsions, J. Dispers. Sci. Technol. 7 (5) (1986) 543–561.
[43] A.A.D. Meirelles, A.L.R. Costa, R.L. Cunha, The stabilizing effect of cellulose crystals in O/W emulsions obtained by ultrasound process, Food Res. Int. 128 (2020), 108746.
[44] J. Araki, M. Wada, S. Kuga, T. Okano, Flow properties of microcrystalline cellulose suspension prepared by acid treatment of native cellulose, Colloids Surf. A Physicochem. Eng. Asp. 142 (1) (1998) 75–82.

[45] F. Hemmati, S.M. Jafari, R.A. Taheri, Optimization of homogenization-sonication technique for the production of cellulose nanocrystals from cotton linter, Int. J. Biol. Macromol. 137 (2019) 374–381.
[46] G.d.F. Furtado, M. Michelon, D.R.B. de Oliveira, R.L. da Cunha, Heteroaggregation of lipid droplets coated with sodium caseinate and lactoferrin, Food Res. Int. 89 (Part 1) (2016) 309–319.
[47] H. Chang, J. Luo, A.A. Bakhtiary Davijani, A.-T. Chien, P.-H. Wang, H.C. Liu, S. Kumar, Individually dispersed wood-based cellulose nanocrystals, ACS Appl. Mater. Interfaces 8 (9) (2016) 5768–5771.
[48] R.R. Lahiji, X. Xu, R. Reifenberger, A. Raman, A. Rudie, R.J. Moon, Atomic force microscopy characterization of cellulose nanocrystals, Langmuir 26 (6) (2010) 4480–4488.
[49] S. Hedjazi, S.H. Razavi, A comparison of Canthaxanthine Pickering emulsions, stabilized with cellulose nanocrystals of different origins, Int. J. Biol. Macromol. 106 (2018) 489–497.
[50] M.S. Mohaiyiddin, O.H. Lin, W.T. Owi, C.H. Chan, C.H. Chia, S. Zakaria, A.R. Villagracia, H.M.J.C.T. Akil, E. Policy, Characterization of Nanocellulose Recovery From *Elaeis guineensis* Frond for Sustainable Development, 18(8), 2016 2503–2512.
[51] S. Naduparambath, J. T.V, S. V, S. M.P, A.K. Balan, P. E, Isolation and characterisation of cellulose nanocrystals from sago seed shells, Carbohydr. Polym. 180 (Supplement C) (2018) 13–20.
[52] J.P.S. Morais, M.d.F. Rosa, M.d.s.M. de Souza Filho, L.D. Nascimento, D.M. do Nascimento, A.R. Cassales, Extraction and characterization of nanocellulose structures from raw cotton linter, Carbohydr. Polym. 91 (1) (2013) 229–235.
[53] A. Gomes, A.L.R. Costa, R.L. Cunha, Impact of oil type and WPI/tween 80 ratio at the oil-water interface: adsorption, interfacial rheology and emulsion features, Colloids Surf. B: Biointerfaces 164 (2018) 272–280.
[54] A. Gomes, A.L.R. Costa, F. de Assis Perrechil, R.L. da Cunha, Role of the phases composition on the incorporation of gallic acid in O/W and W/O emulsions, J. Food Eng. 168 (2016) 205–214.
[55] W.W. Mwangi, K.-W. Ho, B.-T. Tey, E.-S. Chan, Effects of environmental factors on the physical stability of Pickering-emulsions stabilized by chitosan particles, Food Hydrocoll. 60 (2016) 543–550.
[56] I. Capron, B. Cathala, Surfactant-free high internal phase emulsions stabilized by cellulose nanocrystals, Biomacromolecules 14 (2) (2013) 291–296.
[57] E.K. Silva, A.L.R. Costa, A. Gomes, M.A. Bargas, R.L. Cunha, M.A.A. Meireles, Coupling of high-intensity ultrasound and mechanical stirring for producing food emulsions at low-energy densities, Ultrason. Sonochem. 47 (2018) 114–121.
[58] A.G. Cunha, J.-B. Mougel, B. Cathala, L.A. Berglund, I. Capron, Preparation of double Pickering emulsions stabilized by chemically tailored nanocelluloses, Langmuir 30 (31) (2014) 9327–9335.
[59] M. Gestranius, P. Stenius, E. Kontturi, J. Sjöblom, T. Tammelin, Phase behaviour and droplet size of oil-in-water Pickering emulsions stabilised with plant-derived nanocellulosic materials, Colloids Surf. A Physicochem. Eng. Asp. 519 (2017) 60–70.
[60] L. Bai, S. Lv, W. Xiang, S. Huan, D.J. McClements, O.J. Rojas, Oil-in-water Pickering emulsions via microfluidization with cellulose nanocrystals: 1. Formation and stability, Food Hydrocoll. 96 (2019) 699–708.
[61] Z. Hu, S. Ballinger, R. Pelton, E.D. Cranston, Surfactant-enhanced cellulose nanocrystal Pickering emulsions, J. Colloid Interface Sci. 439 (2015) 139–148.
[62] W. Wang, G. Du, C. Li, H. Zhang, Y. Long, Y. Ni, Preparation of cellulose nanocrystals from asparagus (Asparagus officinalis L.) and their applications to palm oil/water Pickering emulsion, Carbohydr. Polym. 151 (2016) 1–8.
[63] S. Fujisawa, E. Togawa, K. Kuroda, Nanocellulose-stabilized Pickering emulsions and their applications, Sci. Technol. Adv. Mater. 18 (1) (2017) 959–971.